Available online at www.sciencedirect.com

ScienceDirect

Current Opinion in Electrochemistry

Review Article

Recent enterprises in high-rate monolithic photo-electrochemical energy harvest and storage devices

Daniel Turner, Ming Li, David Grant and Oluwafunmilola Ola

Abstract

Solar energy is set to play a major role in decarbonising the economy and creating a zero-emissions future. However, there is a need to store this abundant energy and, in many instances, supply that energy at a high rate. With large expense and efficiency losses in integration through external circuits, a monolithic two-electrode harvest storage device or photo-supercapacitor with a high-power density and stable life cycles is an exciting challenge. Here we review the most recent advancements in photo-supercapacitors and some approaches to overcoming various challenges to delivering a marketable device.

Addresses

Advanced Materials Research Group, Faculty of Engineering, The University of Nottingham, University Park, Nottingham, NG7 2RD, United Kingdom

Corresponding author: Ola, Oluwafunmilola (Oluwafunmilola.Ola@nottingham.ac.uk)

Current Opinion in Electrochemistry 2023, **38**:101243

This review comes from a themed issue on **Batteries and Supercapacitors** (2023)

Edited by **Kenneth Ozoemena**

For a complete overview see the Issue and the Editorial

Available online 9 February 2023

https://doi.org/10.1016/j.coelec.2023.101243

Introduction

Recently the investigations into renewable energy sources have increased due to the well-known problems associated with the reliance on finite fossil fuels. One of the forerunning renewable energy sources is solar, which is not surprising with $\sim 739 kWm^{-2}$ incident on the Earth at the surface from the Sun [1,2]. With the power conversion efficiency (PCE) of solar cells rising year on to the point of over 20% for many cell types, the technology has improved greatly [3]. However, due to the intermittence of the Sun storage solutions are necessary. While being possible to couple harvest and storage devices via external circuitry, this is expensive and inefficient. Thus, the investigation into integrated photo-electrochemical energy storage technology has been extensive in the latter days [4–11]. Electrochemical energy storage devices (EESD) work via Faradaic processes, in secondary batteries these processes are slow, and diffusion controlled (minutes to hours), while in supercapacitors (SC) the processes are surface bound and fast (well under a second to a minute) or based on the non-Faradaic electric double layer (EDL) at the electrode electrolyte interface. It is possible to become confused about where the battery/SC line is drawn and sometimes an electrode material or device is reported as an SC while displaying more battery like behaviour being more suitable to the category of high-rate electrochemical (HREC) or supercapattery electrode [12,13]. Despite the publication of excellent discourses on the correct way to report [12,14,15], there are reports of so-called "pseudo-capacitive" materials detailing high specific capacitance and related energy and power while they display non-linear Nernstian or battery like qualities [16–19]. Notwithstanding, it must be pointed out, possibly inflated energy capacity of these devices/materials, the fact remains that the charge capacity increases with illumination thus making them viable candidates as photoelectrode material for high-rate photo-electrochemical storage devices. For a material with a capacitive rectangular CV curve eq. (1) can be used to find specific capacitance (C_s) in F/g; for a non-capacitive CV, specific charge (Q_s) in C/g can be found from eq. (2).

$$C_s = \frac{\int_{V1}^{V2} I(V)dV}{m \cdot \Delta V \cdot \nu} \quad \text{eq.1}$$

$$Q_s = \frac{\int_{V1}^{V2} I(V)dV}{2 \cdot m \cdot \nu} \quad \text{eq.2}$$

Where $\int I(V)dV$ is the area enclosed by the CV curve, m is the active mass of the electrode material, ΔV is the potential window and ν is the sweep rate [5,12,14,15,20–22]. Using the discharge of the GCD of a material can give C_s (eq. (3) or Q_s (eq. (4).

$$C_s = \frac{I \cdot \Delta t}{m \cdot \Delta V} \quad \text{eq.3}$$

$$Q_s = I \cdot \frac{\Delta t}{m} \qquad \text{eq.4}$$

Where m is the mass or area of active material (g); I is the current; Δt is the time of discharge (s); and ΔV the potential window (V). A good example of Faradaic capacitance was reported by Chen et al. using $Ni(HO)_2$ storage material coupled with TiO_2 that displayed a near linear GCD and C_s of 22.9 mF/cm^2, showing good "Pseudocapacitance" [12,23].

The EESDs that include SCs and HRECs or "supercapatteries" are possibly the most important energy storage devices with advantages of high-power density from fast charge/discharge rates, long and stable cycle life from the absence of phase change of electrode material, and often at relatively low cost, potentially using "green" chemistry [12,24]. Herein we concentrate on the most recent developments in the field of so-called photo-supercapacitors (PSC) that lend themselves to applications such as mobile devices, devices on the IOT, wearable devices for fitness and medical sensors or integrated into zero emission buildings (ZEB) [25–32].

Architecture, mechanisms, and applications

There are several different architectures for fully monolithic integrated devices. One of the main characteristic distinctions is the number of current carrying electrodes (CCE), generally two or three [4]. There will be CCEs attached to a photoelectrode or photovoltaic (PV) and counter electrode in a two-electrode device with various charge storage mechanisms involving the electrodes and electrolyte, Fig. 1 a. While in a three-electrode device, there will be a bridging CCE (BCCE) between the counter electrode of the harvesting device and one of the storage element electrodes in either a uniaxial Fig. 1 C or biaxial configuration, Fig. 1 b.

While a two-electrode device has benefits due to the cost and weight of the electrode material being the greatest expense, a three-electrode device is easier to configure as existing technology can be used with a suitable low-resistance BCCE. For the photo-energy capture element, PV, dye-sensitised solar cell (DSSC) and organic semiconductor solar cell (OSSC) can be used; for the storage element the easy-to-configure and fabricate, symmetric electric double layered capacitors (EDLC) return favourable and low-cost results [33–36]. However, the use of a symmetric Pseudocapacitor reportedly returns higher capacitance (Table .1). Das et al. in one instance used a polymer PAAQ as both CE and SC electrodes. To increase charge transport in CE they incorporated CoTe nano-rods while the SC electrodes were naked and suffered from swelling via redox reactions. Subsequently, they used a different polymer PProDOT decorated with Bi nanoflakes and carbon microspheres to prevent swelling and increase charge transport [37,38]. To increase the stability and reduce the mass of the device all devices reported of late used gel electrolyte, this also negates the need for separate packaging and removes the issues of liquid electrolyte leakage. The BCCEs used, range from ITO coated glass, FTO coated glass, carbon fabric, and nickel-foam for devices in a biaxial configuration while Berestok et al. used a conductive epoxy for devices in a uniaxial configuration [33–38]. Using PET electrode/substrate material coupled with flexible OSCs can reduce mass and volume while creating a flexible device with a thickness of as little as 43 microns. Liu et al. and Qin et al. used different SC storage parts, polymer CNT mix and MXene respectively. Qin reported massive volumetric capacitance (Table .1) due to the thinness of material; both devices showed great promise as the basis of self-powering flexible wearables [39,40].

The greatest challenge with a two-electrode configuration is finding a multifunctional electrode material that efficiently harvests, separates, and stores charge. In the search for a photo-sensitive capacitance electrode material, several use a transition metal oxide (TMO) as they show good stability, are relatively cheap, abundant and pose few environmental issues in comparison with e.g., lead containing hybrid perovskite [41–44]. The investigation of hybrid materials and the junctions within promises to offer an answer to the challenge. Momeni et al. investigated the effectiveness of a different TMO deposited to assist the already well-performing $WTiO_2$ nanotube arrays as a photo-assisted supercapacitor. The metal oxides they chose were the well reported alternatives to the problematic but high performing RuO_2; V_2O_5 and MnO_2 [45,46]. The addition of TMO not only shifts the bandgap into the visible spectrum but also reportedly increased surface area and behaved as excellent charge storage sites [44]. The materials' synthesis route affects the morphology and thus its' efficiency as shown by Chatterjee et al. and Altaf et al. The latter found lower crystal dimension and fewer defects causing a greater increase in Coulombic efficiency under illumination while the former found a smaller particle size aided in transport of ions for storage [42,47] Further to the use of transition metals within electrodes is the use of metal ion, i.e. Zn or Mg, in PSC electrolyte explored by Boruah et al. with either photocathode or photoanode storing appropriate ions on charging [48–50]. Isaqu et al. demonstrated the successful use of Bi_2S_3 as sensitizer in DSSC, CE and storage element in a device finding the addition of MWCNT gave better electrocatalytic behaviour and reversibility, with reduced electrode/electrolyte resistance, higher conductivity and faster ion diffusion leading to superior catalytic activity [51]. Investigating the charge storage mechanism of organometallic-halide perovskite PSC (methylammonium bismuth iodide) Popoola et al. using an altered Dunn's equation (*eq.* 5), to include light-induced current in CV scan (*eq.* 6), found the light-induced current fell from 99 to 78% at a rate of

0.01−0.50 V/s respectively showing very strong light-induced energy storage mechanism [12,15,47,52].

$$I_D(V)\Big/\nu^{\frac{1}{2}} = c_1\left(\nu^{\frac{1}{2}}\right) + c_2 \qquad \text{eq.5}$$

Where $I_D(V)$ is the current at a specific potential, $\nu^{\frac{1}{2}}$ is the square root of the scan rate while, c_1 (the surface-bound current) and c_2 (diffusion controlled current) can be found, by plotting, as the intercept and gradient for that potential at that scan rate.

$$I_{mD}(V) = I_D(V) + \chi(\nu) \qquad \text{eq.6}$$

Where $I_{mD}(V)$ is the light modified current and $\chi(\nu)$ is the light induced current. While this is illuminating, going forward it may be interesting to probe the diffusion and surface ratio of current around the max light induced

Figure 1

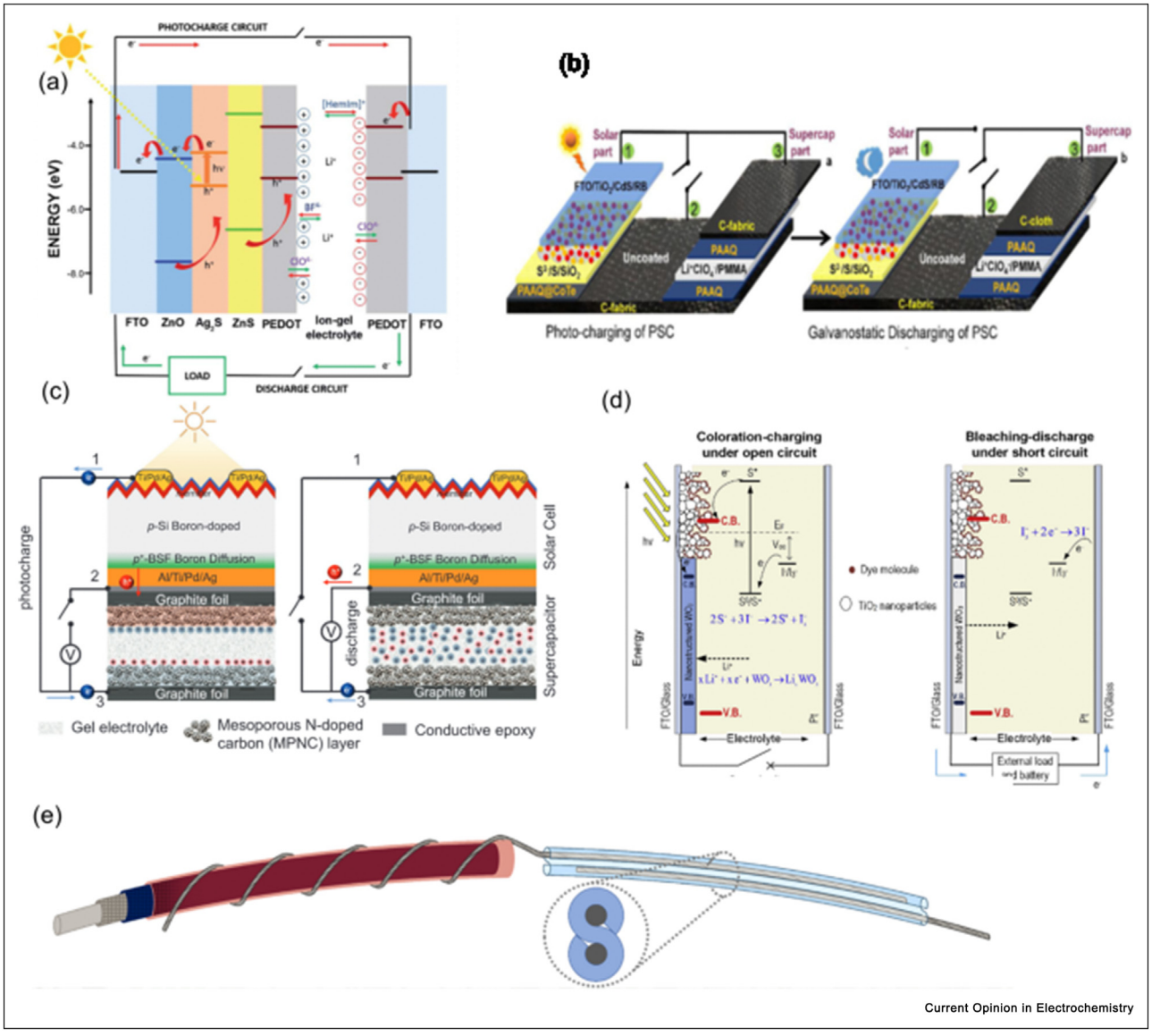

Various PSC device architectures ***(a)*** *two-electrode planar uniaxial strategy based on a heterojunction PV and symmetric SC showing charge transfer route. Reproduced with permission from Ref.* [43] *Creative Commons.* ***(b)*** *A three-electrode biaxial parallel planar strategy based on DSSC and symmetric SC. Reproduced with permission from Ref.* [38] *Copyright Elsevier. The charge discharge path of a uniaxial 3 electrode device with p-n junction incorporating symmetric supercapacitor. Reproduced with permission from* Ref. [34] *Creative Commons* ***(d)*** *photo-chargeable electrochromic energy-storage device utilising nanostructured WO_2 as charge storage and light shading element in a smart window. Reproduced with permission from Ref.* [31] *Copyright Elsevier.* ***(e)*** *Fibre type device with the counter electrode of the DSSC harvest element utilised as one of the storage element electrodes. Reproduced with permission from Ref.* [26] *Creative Commons.*

Table 1

Storage capacity performance, harvesting and device efficiency with reported stability data of three-electrode devices.

Device configuration	Photo active element	Capacitor electrodes and [electrolyte]	Capacitance	Overall device efficiency (%)	Energy capacity	Power capacity	PCE (%)	Cycle stability (%)	Ref.
Biaxial	DSSC (TiO_2/CdS/RB (Rose Bengal dye))	PAAQ/carbon fabric [$LiClO_4$/PMMA gel]	53 F/cm^2 @ 0.5 mA/cm^2	4.68	5 × 10^{-6} Wh/cm^2	0.4 × 10^{-3} W/cm^2	8.25		[38]
Biaxial	DSSC (SnO_2 Kokum)	graphene (LASER treated Kapton) [BPE (PVP PVA)]	20 F/g				0.56		[35]
Uniaxial	HOIP (Formamadinium-$CsPb(IBr)_3$)	MPNCs/dense carbon[PVA/H_2SO_4/H_2O (gel)]	400 F/g @ 0.5 A/g (31-11 mF/cm^2)	11.5 @ 0.5 mA/cm^2	13.8 Wh/kg (10.41 μWh/cm$^-$) @	117.64 W/kg (88.23 μW/cm^2)	12.5		[33]
Uniaxial	SSC (Si p$^-$p+ boron doped)	MPNCs/dense carbon[PVA/H_2SO_4/H_2O (gel)]	224 F/g @ 0.5 A/g (47-18 mF/cm^2)	11.80	7.7 Wh/kg @	71 W/kg	20.5	Capacitance 94% Coulombic 95% after 5000 cycles	[34]
Biaxial	OSC (ITO/SnO_2/Cs_2CO_3/ P3HT:PC60BM/ MoO_3/Ag)	MWCNT[PVA/H_3PO_4]	20 F/g @ 0.035 A/g	2.27	0.81 Wh/kg @	125 W/kg	3.57	Nearly 100% for 4000 cycles	[36]
Biaxial	DSSC TiO_2/SNGP/ CdS: [S^{2-}/S gel]: PProDOT:CMS-BiNF	PProDOT/CMS-BiNF [Li^+-gel]	104.6 mF/cm^2	6.8	9 μWh/cm^2	0.026 mW/cm^2	9.4	Stable over 50 cycles	[37]
Uniaxial (flexible)	OSC (ZnO/ (PBDTTT-OFT)/ ($PC_{71}BM$)/.MoO_x)	PEDOT:PSS/CNT [H_2SO_4:PVA(gel)]	273 mF/cm^2	5.92	–	–	9.73	96% efficiency after 100 cycles	[40]
Uniaxial (flexible)	OSC (PM6:Y6)	$Ti_3C_2T_x$ [ionogel]	502 F/cm^3	Storage 2.2	–	–	2.5 (frontlit) 1.89 (backlit)	95% capacitance after 10,000 cycles	[39]

Abbreviations: PAAQ – poly (1-aminoanthraquinone), PMMA – Poly(methyl methacrylate), BPE – blend polymer electrolyte, PVP – Polyvinyl pyrrolidone, PVA – Poly(vinyl alcohol).
HOIP – halide organic inorganic perovskite, MPNC – mesoporous nano-carbons, P3HT – poly (3-hexylthiophene-2,5-diyl), PC60BM – phenyl C60-butyric acid methyl, MWCNT – many walled carbon nano-tubes, SNGP – Sulphur and nitrogen doped graphene particles, PProDOT – poly(3,4-propylenedioxythiophene), CMS – carbon micro-spheres, BiNF – bismuth nano-flakes.
PBDTTT-OFT – poly[4,8-bis(5-(2-ethylhexyl)thiophen-2-yl)benzo[1,2-b; 4,5-b′]dithiophene-2,6-diyl-alt-(4-octyl-3-fluorothieno[3,4-b]thiophene)-2-carboxylate-2-6-diyl], $PC_{71}BM$ – [6,6]-phenyl-C_{71}-butyric acid methyl ester, PEDOT – Poly(3,4-ethylenedioxythiophene), PSS – polystyrene sulfonate, PM6 – Poly[(2,6-(4,8-bis(5-(2-ethylhexyl-3-fluoro)thiophen-2-yl)-benzo[1,2-b:4,5-b']dithiophene))-alt-(5,5-(1′,3′-di-2-thienyl-5′,7′-bis(2-ethylhexyl)benzo[1′,2′-c:4′,5′-c']dithiophene-4,8-dione)], Y6 – Non fullerene acceptor Y6 ($C_{82}H_{86}F_4N_8O_2S_5$).

current scan rate at various power densities of illumination. It is also important to note this doesn't discern between the Faradaic and non-Faradaic processes at the surface.

To further improve device efficiency, internal resistance on discharge due to junction or Schottky barriers needs to be addressed [53,54]. Interrogation of charge separation, transport and storage mechanisms are important to better understand devices and achieve higher efficiencies. Wenjun et al. investigated and reported on the concept of a Faradaic junction, a mechanism by which there is an exchange of electrons and ions at a Faradaic material (farador) electrolyte interface during a photo-excitation within a semiconductor interfaced with a farador. The charge carriers are therefore a mix of both with the ionic charge being stored in the farador at or on the surface. By blocking the short circuit between the farador and the CCE by the judicious use of a semiconductor, capacitance is increased with a negligible potential barrier between the farador and short-circuited CCE but the potential window of the farador is affected by the Fermi level of the semiconductor. This barrier height can be controlled by the band position of the semiconductor (Fig. 2 a) [54]. Two junctions in a planar sandwich configuration were fabricated, one with WO_3 and the other with $MoO_{2.5}$, photo-electrodeposited on n^+p-Si substrate. Comparing the photo charge and dark discharge activity of the junctions with that of the same deposited on carbon substrates, it was shown, the potential window can be shifted by a semiconductor while maintaining the dis/charge behaviour. The first 2-electrode photo-supercapacitor that can discharge without an applied bias via the adjusting potential was devised, evidenced by experimental CV plots [55]. They used the theory of faradaic junction to explain greater than theoretical open circuit potential (OCP) of semiconductor/semiconductor interfaces such as quantum dot sensitised solar cells or perovskite solar cells and high photovoltages. In situ techniques were used to support the theory that the junction promotes photo-driven surface Faradaic reactions within TiO_2/CdS on the TiO_2 surface only, due to the potential window favouring the Faradaic charge/discharge process on TiO_2. This reaction seemingly occurred only on the surface not in the bulk and was promoted by the swift charge transfer between the TiO_2 and the CdS [56]. Subsequently, a two-electrode photo-rechargeable Faradaic junction device was created, which exhibited a photovoltage memory effect; the discharge voltage matching that of the photovoltage which in turn promotes high performance. This effect didn't occur with all CEs while probing the effect via a real-time OCP measurement method; the OCP (between SCE and working electrode) for the photoelectrode (PE) and the CE in a disconnected dark stage, a connected dark stage, a connected light stage and back to a disconnected dark stage. It was apparent

Figure 2

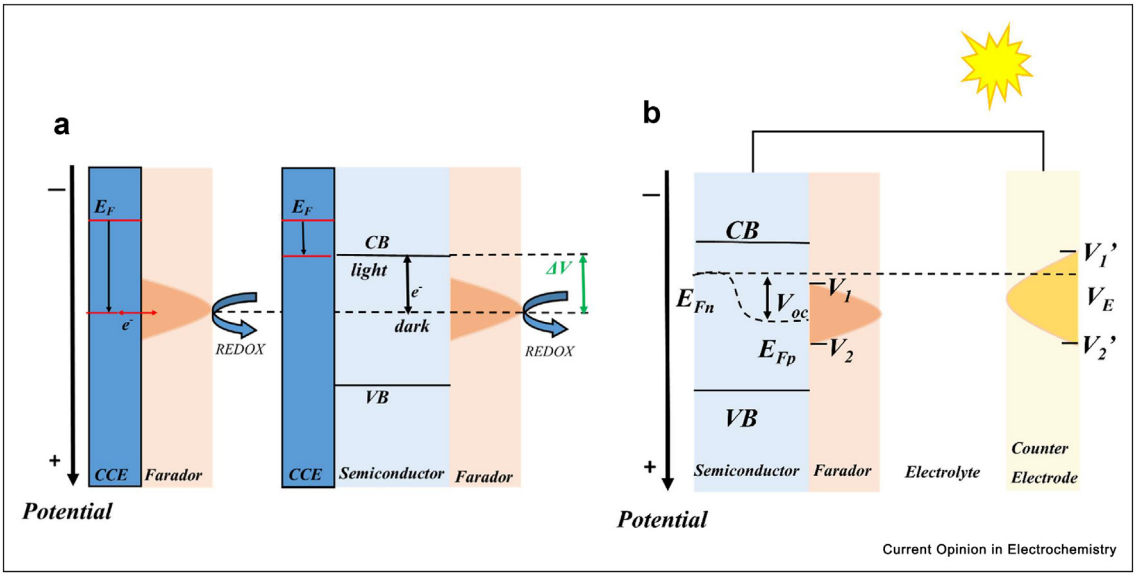

a. Band diagrams of the interfaces between current carrying electrode (CCE)/Faradaic layer (farador)/electrolyte; and CCE/semiconductor/farador/electrolyte under an applied potential. ΔV is the barrier height created by eliminating the short circuit between farador and CCE, with the choice of semiconductor (band gap) and farador (redox potential) tuning the barrier [54]. **b.** Schematic of working prerequisite for the photovoltage memory effect in a solar rechargeable device. V_1 and V_2 are a lower and upper limit of Faradaic potential window of a Faradaic material in a photoelectrode, respectively; V_1' and V_2' are a lower and upper limit of Faradaic potential window of a counter electrode, respectively; V_E is an equilibrium potential of a counter electrode. V_{oc} is a photovoltage in a photoelectrode. To realize a photo-oxidization of a Faradaic material on a semiconductor, the hole quasi-Fermi level (E_{Fp}) in a semiconductor should be more positive than V_1 and more negative than V_2, that is, $V_1<V_E + V_{oc}<V_2$. On the other hand, if photo-generated electrons from a semiconductor can reduce the Faradaic layer, not the electric double layer of a counter electrode, V_E should be more positive than V_1' and more negative than V_2' ($V_1'<V_E<V_2'$) Wang et al. 2022 [57].

Table 2

Storage capacity performance, device efficiency and reported stability data of two-electrode devices.

Device Configuration	Photo active element	Counter electrode	Electrolyte	Capacitance	Power capacity	Maximum charging voltage (V)	Cycle Stability	Ref.
Planar	$ZnO/Ag_2S/ZnS$	PEDOT	PVP $HEMIm/BF_4$ (ionic gel)	0.667 mF/cm^2	–	0.33	~98% after 1200 cycles	[43]
Planar	Si/WO_3	Carbon	H_2SO_4 (aq)	Capacity (8.6 mC/cm^2)	0.8 mW/cm^2	–	–	[55]
Planar	TiO_2/Bi_2S_3	Bi_2S_3/MWCNT	I^{3-}/I^-	133.6/g	1992/kg	–	>80% after 3000 cycles	[51]
Planar	Methylamonium Bismuth triodide	Methylamonium Bismuth triodide	CPH-G gel (PVA Chlorobenzene H_3PO_4)	0.28 mF/cm^2 0.35F/g @ 0.01V/s	–	–	94.79% after 5000 cycles	[52]
Planar	g-C_3N_4@rGO/FTO	Zn	$ZnSO_4$	11.4 F/g at 5.0 mA/g	1625 W/kg @ 5 mA/g 16,250 W/kg @ 50 mA/g	0.85	90% after 1000 cycles	[48]
Planar	Vanaduium Pentoxide (V_2O_5)	Activated Carbon	$Zn(CF_3SO_3)_2$	138 F/g	–	0.5	99% after 4000 cycles	[49]
Planar	$BiVO_4$/CoPi	Carbon cloth	Potassium phosphate buffer (KPi)	–	–	0.88	–	[59]
Planar	$WTiO_2$ NT MnO_2/ $V_2O_5/MnO_2.V_2O_5$	$WTiO_2$ NT MnO_2/ $V_2O_5/MnO_2.V_2O_5$	1M LiCl	95 mF/cm^2 at 0.12 mA/cm^2 (237.6F/g at 6.0 A/g)	39.96 mW/cm^2 (360 W/kg)	0.5	94% and 93% capacitance retention in light and dark respectively after 5000 cycles	[44]
Planar	$BiVO_4$-rGo	rGo	Na_2SO_4	141.8 F/g @ 0.2 A/g	–	–	78% retention after 100 cycles	[60]
Fibre/Strip	OSC (TCE/ZnO/ PTB7-Th:$PC_{71}BM$/ PEDOT:PSS/Ag)	rGO-PEDOT:PSS	PVA/LiCl gel	52 mF/cm^2	–	–	96% capacitance after 5000 GCD cycles 95% capacitance after 1000 bending cycles	[32]
Fibre	DSSC (TiO_2 N719)	CNTYarn (p {$FeCl_3$} doped)	Li-TFSI film	78.3 mF/cm^2	–	–	90% after 500 bending cycles and 10 washing cycles	[26]

Abbreviations: $HEMIm/BF_4$ – 1-(2-hydroxyethyl)-3-methyl imidazolium tetrafluoroborate, rGO – reduced graphene oxide, TCE – transparent conductive electrode, PTB7-Th – Poly[4,8-bis(5-(2-ethylhexyl) thiophen-2-yl)benzo[1,2-b;4,5-b']dithiophene-2,6-diyl-alt-(4-(2-ethylhexyl)-3-fluorothieno[3,4-b]thiophene-)-2-carboxylate-2-6-diyl)], CNTY – carbon nanotube yarn.

"side reactions" occurring under zero bias were trivial and lead to 100% Coulombic efficiency over 80 cycles also proving excellent reversibility. Due to the photovoltage memory effect, a higher performance occurred from "increased storage time and higher charge quantity of the faradaic layer than the electric double layer". With the careful choice of semiconductor, farador and CE the onset potential, photovoltage and discharge voltage can be controlled (Fig. 2 b). The discovery of the mechanism of tuning semiconductor band gap and Fermi level to farador equilibrium potential and Faradaic potential window along with the CE equilibrium potential and Faradaic potential window is key to designing high energy-dense two-electrode devices [57].

An important application of PSCs will be in zero emission buildings (ZEB). There have been several recent investigations into this application. Orozco-Messana et al. investigated a heterojunction PV coupled with a SC incorporated within a porous stoneware tile as near ZEB material [29]. They decided on a TMO heterojunction PV as the "best compromise" between efficiency, simplicity and durability. The storage element was a modified rGO with pseudocapacitive $Ni(OH)_2$ coupled with an electroless deposited conductive layer of Ni−Mo−P as an adherence agent to the porous porcelain substrate. The conductive layer showed good adhesion for the metal layer and low resistivity of 7.2 MPa and 10.6 μΩ cm respectively. They recorded good capacitive stability over 200 cycles [30]. Photo-electrochromic capacitors (PESC) as smart windows to regulate a building's temperature and light ingress with solar energy capture/storage have been investigated [25,28,29,31]. TiO_2 based DSSC were commonly used to charge with the redox action of electrochromic WO_3 to store energy as intercalated ions balancing the negative excitons from the DSSC causing the darkening (Fig. 1 d. [31]). Yin et al. successfully overcame the limiting diffusion speed and electrolyte driven corrosion of the electrode by incorporating WS_2, the further inclusion in the DSSC CE also increased conductivity. Not only did the stored energy drive the electrochromic action but could be used on discharge for external load [25]. Liu et al. also produced a PESC complimented with Prussian blue dye. The combination of electrochromic chemicals gave a multimodal material working in original, bright, cool and dark modes. As a future development of this excellent technology the driving potential to trigger the Dark mode, for total blockage of light and heat, could be better supplied from the stored photo-charge [28]. Zhang et al. reported on a flexible PESC; the conductive contact substrate was ITO-PET which shows low sheet resistance and high transmittance. Its flexibility allows for smart windows of all shapes and wearable applications [29]. An alternative route to wearables is fibres; Jin et al. used an existing printing technique to embed metal strips into a UV-curable conducting polymer creating a stable, flexible OSC SC strip device that was then woven into a textile [32]. Another investigation into a fibre style PSC came from Kim et al. using a novel method of "floating catalyst" CVD [58] to create threads of CNT that were subsequently spun into yarn and then appropriately doped. The device showed great stability even after 10 cycles of automatic washing (Table 2) [26]. These kinds of application innovations certainly bring us one step closer to marketable devices, a comparison of storage capacity and stability of recent two-electrode devices can be seen in Table 2.

Conclusion

In reviewing the most recent advancements in the area of PSCs we covered the importance of standardisation of characterisation parameters and definitions, with the inclusion of standard characterisation methods CV, GCD with appropriate analysis to avoid confusion. The efficiency, capacity, stability and cost of materials and processes need to be overcome before the commercial viability of PSCs is realised. We have seen some of these issues tackled by the reduction of device mass through two electrode configurations, reduction of material mass and volume and the use of more stable elements such as gel electrolyte and TMO based electrodes. Using existing fabrication techniques such as printing, and the creation of new fabrication techniques move us closer to achieving marketable products. By more fully understanding both the mechanisms of charge transfer and storage through novel in-situ techniques and material structure performance relationships, we can increase device efficiency further.

Declaration of competing interest

The authors declare that they have no known competing financial interests or personal relationships that could have appeared to influence the work reported in this paper.

Data availability

No data was used for the research described in the article.

Acknowledgements

This work was supported by the University of Nottingham (Research Fellowship, A7X164).

References

1. Chen Julisan, Chen J, Oliver LM: *(PDF) Physics of Solar Energy-Academia.edu*. Hoboken: Wiley; 2011. https://www.academia.edu/77101822/Physics_of_Solar_Energy_J_Chen_. Accessed 4 August 2022.

2. Gawusu S, Zhang X, Ahmed A, Jamatutu SA, Miensah ED, Amadu AA, Osei FAJ: **Renewable energy sources from the perspective of blockchain integration: from theory to application**. *Sustain Energy Technol Assessments* 2022, **52**, 102108, https://doi.org/10.1016/j.seta.2022.102108.

3. NREL, Best: ***Research-cell efficiency chart***. https://www.nrel.gov/pv/assets/pdfs/best-research-cell-efficiencies-rev220126 pdf. Accessed 11 August 2022.

4. Fagiolari L, Sampò M, Lamberti A, Amici J, Francia C, Bodoardo S, Bella F: **Integrated energy conversion and storage devices: interfacing solar cells, batteries and supercapacitors**. *Energy Storage Mater* 2022, https://doi.org/10.1016/j.ensm2022.06.051.

5. Manopriya S, Hareesh K: **The prospects and challenges of solar electrochemical capacitors**. *J Energy Storage* 2021, **35**, 102294, https://doi.org/10.1016/J.EST.2021.102294.

6. Devadiga D, Selvakumar M, Shetty P, Santosh MS: **Recent progress in dye sensitized solar cell materials and photo-supercapacitors: a review**. *J Power Sources* 2021, **493**, 229698, https://doi.org/10.1016/j.jpowsour.2021.229698.

7. Sun Y, Yan X: **Recent advances in dual-functional devices integrating solar cells and supercapacitors**. *Solar RRL* 2017, **1**, 1700002, https://doi.org/10.1002/solr.201700002.

8. Meng H, Pang S, Cui G: **Photo-supercapacitors based on third-generation solar cells**. *ChemSusChem* 2019, **12**: 3431–3447, https://doi.org/10.1002/cssc.201900398.

9. Ng CH, Lim HN, Hayase S, Harrison I, Pandikumar A, Huang NM: **Potential active materials for photo-supercapacitor: a review**. *J Power Sources* 2015, **296**:169–185, https://doi.org/10.1016/j.jpowsour.2015.07.006.

10. Rout NKCS: **Photo-powered integrated supercapacitors: a review on recent developments, challenges and future perspectives**. *J Mater Chem A Mater* 2021, **9**:8248–8278, https://doi.org/10.1039/d1ta00444a.

11. Zhang H, Lu Y, Han W, Zhu J, Zhang Y, Huang W: **Solar energy conversion and utilization: towards the emerging photoelectrochemical devices based on perovskite photovoltaics**. *Chem Eng J* 2020, **393**, https://doi.org/10.1016/j.cej.2020.124766.

12. Chen GZ: **Linear and non-linear pseudocapacitances with or without diffusion control**. *Prog Nat Sci: Mater Int* 2021, **31**: 792–800, https://doi.org/10.1016/j.pnsc.2021.10.011.

13. Chen GZ: *Supercapacitor and supercapattery as emerging electrochemical energy stores*. 2016:173–202, https://doi.org/10.1080/09506608.2016.1240914. Http://Dx.Doi.Org/10.1080/09506608.2016.1240914. 62.

14. * Mathis TS, Kurra N, Wang X, Pinto D, Simon P, Gogotsi Y: **Energy storage data reporting in perspective—guidelines for interpreting the performance of electrochemical energy storage systems**. *Adv Energy Mater* 2019, **9**, 1902007, https://doi.org/10.1002/aenm.201902007.

The paper covers the main causes of inaccurate data reporting while showing examples of how researchers should report. They outline how best to measure and communicate the measurements of capacity, efficiencies and impedances they also discuss the differences of capacitive and pseudocapacitive materials. The supporting information includes an excellent checklist for reporting electrochemical storage data.

15. Hussain I, Sahoo S, Mohapatra D, Ahmad M, Iqbal S, Javed MS, Gu S, Qin N, Lamiel C, Zhang K: **Recent progress in trimetallic/ternary-metal oxides nanostructures: misinterpretation/misconception of electrochemical data and devices**. *Appl Mater Today* 2022, **26**, 101297, https://doi.org/10.1016/j.apmt.2021.101297.

16. Pattananuwat P, Khampuanbut A, Haromae H: **Novel electrode composites of mixed bismuth-iron oxide/graphene utilizing for photo-assisted supercapacitors**. *Electrochim Acta* 2021, **370**, 137741, https://doi.org/10.1016/j.electacta.2021.137741.

17. Kajana T, Velauthapillai D, Shivatharsiny Y, Ravirajan P, Yuvapragasam A, Senthilnanthanan M: **Structural and photoelectrochemical characterization of heterostructured carbon sheet/Ag2MoO4-SnS/Pt photocapacitor**. *J Photochem Photobiol Chem* 2020, **401**, 112784, https://doi.org/10.1016/j.jphotochem.2020.112784.

18. Kajana T, Pirashanthan A, Yuvapragasam A, Velauthapillai D, Ravirajan P, Senthilnanthanan M: **Bimetallic AC/Ag2CrO4/SnS heterostructure photoanode for energy conversion and storage: a self-powered Photocapacitor**. *J Power Sources* 2022, **520**, 230883, https://doi.org/10.1016/j.jpowsour.2021.230883.

19. Muthu Kumar A, Ragavendran V, Mayandi J, Ramachandran K, Jayakumar K: **Influence of PVP on Bi25FeO40 microcubes for supercapacitors and dye-sensitized solar cells applications**. *J Mater Sci Mater Electron* 2022, **33**:9512–9524, https://doi.org/10.1007/s10854-021-07471-4.

20. Majumdar D, Mandal M, Bhattacharya SK: **Journey from supercapacitors to supercapatteries: recent advancements in electrochemical energy storage systems**. *Emergent Mater* 2020, **3**:347–367, https://doi.org/10.1007/s42247-020-00090-5.

21. Chodankar NR, Pham HD, Nanjundan K, Fernando JFS, Jayaramulu K, Golberg D, Han Y-K, Dubal DP, Chodankar NR, Han Y-K, Pham HD, Fernando JFS, Golberg D, Dubal DP, Nanjundan AK, Jayaramulu K: **True meaning of pseudocapacitors and their performance metrics: asymmetric versus hybrid supercapacitors**. *Small* 2020, **16**, 2002806, https://doi.org/10.1002/smll.202002806.

22. * Fleischmann S, Mitchell JB, Wang R, Zhan C, Jiang D-E, Presser V, Augustyn V: *Pseudocapacitance: from fundamental understanding to high power energy storage materials*. 2020, https://doi.org/10.1021/acs.chemrev.0c00170.

An extensive review of the field of pseudocapacitance, with an in-depth discussion of the history and current ideas around the definition and mechanisms associated with the phenomenon. Tackling the subject of extrinsic and intrinsic pseudocapacitance and the difference between diffusion-controlled and intercalation-controlled current. A detailed appraisal of recent materials and how to manipulate materials through nanostructuring and atomic scale tuning to increase pseudocapacitance.

23. Chen P, Cao C, Ding C, Yin Z, Qi S, Guo J, Zhang M, Sun Z: **One-body style photo-supercapacitors based on Ni(OH)2/TiO2 heterojunction array: high specific capacitance and ultra-fast charge/discharge response**. *J Power Sources* 2022, **521**, 230920, https://doi.org/10.1016/j.jpowsour.2021.230920.

24. Winter M, Brodd RJ: **What are batteries, fuel cells, and supercapacitors?** *Chem Rev* 2004, **104**:4245–4269, https://doi.org/10.1021/cr020730k.

25. Yin J, Li J, Wang L, Cai B, Yang X, Li X, Lü W: **Integrated photoelectrochromic supercapacitor for applications in energy storage and smart windows**. *J Energy Storage* 2022, **51**, 104460, https://doi.org/10.1016/j.est.2022.104460.

[26]. * Kim JH, Koo SJ, Cheon JY, Jung Y, Cho S, Lee D, Choi JW, Kim T, Song M: **Self-powered and flexible integrated solid-state fiber-shaped energy conversion and storage based on CNT Yarn with efficiency of 5.5**. *Nano Energy* 2022, **96**, 107054, https://doi.org/10.1016/j.nanoen.2022.107054.

The device fabricated from a carbon nanotube yarn and fibre DSSC proved both efficient (4.69% overall energy conversion) and very stable even under 10 cycles of automatic washing. The use of a novel floating vapour CVD method to fabricate the CNT yarn and subsequently dope either n or p with PEI and FeCl3 respectively created a fibre with excellent conductivity and capacitance (78.26 mF cm2) showing great potential in wearable technology.

27. Zeng Q, Lai Y, Jiang L, Liu F, Hao X, Wang L, Green MA: **Integrated photorechargeable energy storage system: next-generation power source driving the future**. *Adv Energy Mater* 2020, **10**, 1903930, https://doi.org/10.1002/aenm201903930.

28. Liu Z, Yang J, Leftheriotis G, Huang H, Xia Y, Gan Y, Zhang W, Zhang J: **A solar-powered multifunctional and multimode electrochromic smart window based on WO3/Prussian blue complementary structure**. *Sustainable Materials and Technologies* 2022, **31**, e00372, https://doi.org/10.1016/j.susmat.2021.e00372.

29. Zhang D, Sun B, Huang H, Gan Y, Xia Y, Liang C, Zhang W, Zhang J: **A solar-driven flexible electrochromic supercapacitor**. *Materials* 2020, **13**:1206, https://doi.org/10.3390/ma13051206. 2020, Vol. 13, Page 1206.

[30]. ** Orozco-Messana J, Daly R, Zanchetta-Chittka IF: **Cu2O–ZnO heterojunction solar cell coupled to a Ni(OH)2-rGO-PPy supercapacitor within a porous stoneware tile**. *Ceram Int* 2020, **46**:24831–24837, https://doi.org/10.1016/j.ceramint.2020.06.229.

The device uses a stable and low maintenance TMO heterojunction as harvest element and bridged to a porous stoneware tile base as a storage element incorporating Ni(OH)2-rGO-PPy composite pushing forward the ideal of a near-zero emissions building. The use of

electroless deposited Ni–Mo–P layer with its excellent adhesion and conductivity worked well to couple the harvest and balanced storage element.

31. Zhang J, Yang J, Leftheriotis G, Huang H, Xia Y, Liang C, Gan Y, Zhang W: **Integrated photo-chargeable electrochromic energy-storage devices**. *Electrochim Acta* 2020, **345**, 136235, https://doi.org/10.1016/j.electacta.2020.136235.

32. Jin W-Y, Mayaji Ovhal M, Beng Lee H, Tyagi B, Kang J-W, Jin W, Ovhal MM, Lee HB, Tyagi B, Kang J: **Scalable, all-printed photocapacitor fibers and modules based on metal-embedded flexible transparent conductive electrodes for self-charging wearable applications**. *Adv Energy Mater* 2021, **11**, 2003509, https://doi.org/10.1002/aenm.202003509.

33. Berestok T, Diestel C, Ortlieb N, Buettner J, Matthews J, Schulze PSC, Goldschmidt JC, Glunz SW, Fischer A: **High-efficiency monolithic photosupercapacitors: smart integration of a perovskite solar cell with a mesoporous carbon double-layer capacitor**. *Solar RRL* 2021, **5**, 2100662, https://doi.org/10.1002/solr.202100662.

34. Berestok T, Diestel C, Ortlieb N, Glunz SW, Fischer A: **A monolithic silicon-mesoporous carbon photo-supercapacitor with high overall photoconversion efficiency**. *Adv. Mater. Technol.* 2022:1–16, https://doi.org/10.1002/admt.202200237.

35. Sangeetha DN, Hegde N, Poojari V, Devadiga D, Sudhakar YN, Santosh MS, Selvakumar M: **Conductivity/electrochemical study of Polyvinyl pyrrolidone-Poly(vinyl alcohol)/I3– thin film electrolyte for integrated dye-sensitized solar cells and supercapacitors**. *J Electron Mater* 2020, **49**:6325–6335, https://doi.org/10.1007/s11664-020-08432-z. 49 (2020).

36. Shin J, Tran VH, Tien Nguyen DC, Kim SK, Lee SH: **Integrated photo-rechargeable supercapacitors formed via electrode sharing**. *Org Electron* 2021, **89**, 106050, https://doi.org/10.1016/j.orgel.2020.106050.

37. Das A, Ojha M, Subramanyam P, Deepa M: **A poly(3,4-propylenedioxythiophene)/carbon micro-sphere-bismuth nanoflake composite and multifunctional Co-doped graphene for a benchmark photo-supercapacitor**. *Nanoscale Adv* 2020, **2**:2925–2942, https://doi.org/10.1039/d0na00103a.

38. Das A, Deshagani S, Ghosal P, Deepa M: **Redox active and electrically conducting cobalt telluride Nanorods/Poly(1-aminoanthraquinone) composite and photoactive Rose Bengal dye based photo-supercapacitor**. *Appl Mater Today* 2020, **19**, 100592, https://doi.org/10.1016/j.apmt.2020.100592.

39. Qin L, Jiang J, Tao Q, Wang C, Persson I, Fahlman M, Persson POA, Hou L, Rosen J, Zhang F: **A flexible semi-transparent photovoltaic supercapacitor based on water-processed MXene electrodes**. *J Mater Chem A Mater* 2020, **8**:5467–5475, https://doi.org/10.1039/d0ta00687d.

40. Liu R, Takakuwa M, Li A, Inoue D, Hashizume D, Yu K, Umezu S, Fukuda K, Someya T: **An efficient ultra-flexible photo-charging system integrating organic photovoltaics and super-capacitors**. *Adv Energy Mater* 2020, **10**, https://doi.org/10.1002/aenm.202000523.

41. Ren Y, Zhu T, Liu Y, Liu Q, Yan Q, Ren YF, Zhu T, Liu YD, Liu QB, Yan QY: **Direct utilization of photoinduced charge carriers to promote electrochemical energy storage**. *Small* 2021, **17**, 2008047, https://doi.org/10.1002/smll.202008047.

42. Altaf CT, Coskun O, Kumtepe A, Rostas AM, Iatsunskyi I, Coy E, Erdem E, Sankir M, Sankir ND: **Photo-supercapacitors based on nanoscaled ZnO**. *Sci Rep* 2022, **12**, 11487, https://doi.org/10.1038/s41598-022-15180-z.

43. Solís-Cortés D, Navarrete-Astorga E, Schrebler R, Peinado-Pérez JJ, Martín F, Ramos-Barrado JR, Dalchiele EA: **A solid-state integrated photo-supercapacitor based on ZnO nanorod arrays decorated with Ag 2 S quantum dots as the photo-anode and a PEDOT charge storage counter-electrode**. *RSC Adv* 2020, **10**:5712–5721, https://doi.org/10.1039/c9ra10635a.

44. Mohsen Momeni M, Mohammadzadeh Aydisheh H, Lee B-K: **Effectiveness of MnO2 and V2O5 deposition on light fostered supercapacitor performance of WTiO2 nanotube: novel electrodes for photo-assisted supercapacitors**. *Chem Eng J* 2022, **450**, 137941, https://doi.org/10.1016/j.cej.2022.137941.

45. Yue T, Shen B, Gao P: **Carbon material/MnO2 as conductive skeleton for supercapacitor electrode material: a review**. *Renew Sustain Energy Rev* 2022, **158**, 112131, https://doi.org/10.1016/j.rser.2022.112131.

46. Li X, Ma Y, Yu Y, Li G, Zhang C, Cao M, Xiong Y, Zou J, Zhou Y, Gao Y: *A flexible Zn-ion hybrid micro-supercapacitor based on MXene anode and V2O5 cathode with high capacitance, vol. 428*. 2022, 130965, https://doi.org/10.1016/j.cej.2021.130965.

47]. Chatterjee M, Saha S, Das S, Pradhan SK: **Advanced asymmetric supercapacitor with NiCo2O4 nanoparticles and nanowires electrodes: a comparative morphological hierarchy**. *J Alloys Compd* 2020, **821**, 153503, https://doi.org/10.1016/j.jallcom2019.153503.

48]. Boruah BD, Mathieson A, Wen B, Jo C, Deschler F, de Volder M: **Photo-rechargeable Zinc-ion capacitor using 2D graphitic carbon nitride**. *Nano Lett* 2020, **20**:5967–5974.

49]. * Boruah BD, Wen B, Nagane S, Zhang X, Stranks SD, Boies A, de Volder M: **Photo-rechargeable Zinc-ion capacitors using V2O5-activated carbon electrodes**. *ACS Energy Lett* 2020, **5**:3132–3139, https://doi.org/10.1021/acsenergylett.0c01528. https://doi.org/.

The device showing a photo-rechargeable Zn ion capacitor using V2O5 and silver nanowires as conductive additives had increased capacitance under illumination (~63%) and excellent stability of 99% retention after 4000 cycles. They found from time-resolved photoluminescence data that the carrier lifetimes increased with the addition of the silver nanowires by ~40%. They reported the simultaneous discharging to load and photo-charging and measured a capacity of ~48 mF cm-2 at a discharge current of 0.1 mA and a photo-charged energy density of 1.67 μWh cm-2.

[50]. Park SK, Boruah D, Pujari A, Kim B-M, de Volder M: **Photo-enhanced magnesium-ion capacitors using photoactive electrodes**. *Small* 2022, 2202785, https://doi.org/10.1002/smll.202202785.

[51]. Isaqu JP, Vnekatesan R, Nagalingam Rajamanickam, Mayandi J: **, | Nithiananthi Perumal, S. Bi, Bi2S3 can do it all: sensitizer, counter electrode, and supercapacitor for symmetric solar cell assisted photo-supercapacitor**. *Int J Energy Res* 2022, https://doi.org/10.1002/er.7908.

[52]. Popoola IK, Gondal MA, Popoola A, Oloore LE: **Bismuth-based organometallic-halide perovskite photo-supercapacitor utilizing novel polymer gel electrolyte for hybrid energy harvesting and storage applications**. *J Energy Storage* 2022, **53**, 105167, https://doi.org/10.1016/j.est.2022.105167.

[53]. Murakami TN, Kawashima N, Miyasaka T: **A high-voltage dye-sensitized photocapacitor of a three-electrode system**. *Chem Commun* 2005, **0**:3346–3348, https://doi.org/10.1039/b503122b.

[54]. Chen X, Zhu K, Wang P, Sun G, Yao Y, Luo W, Zou Z: **Reversible charge transfer and adjustable potential window in semiconductor/faradaic layer/liquid junctions**. *iScience* 2020, **23**, 100949, https://doi.org/10.1016/j.isci.2020.100949.

[55]. Wang P, Chen X, Sun G, Wang C, Luo J, Yang L, Lv J, Yao Y, Luo W, Zou Z: **A capacitor-type faradaic junction for direct solar energy conversion and storage**. *Angew Chem Int Ed* 2021, **60**:1390–1395, https://doi.org/10.1002/anie.202011930.

[56]. Chen M, Dong H, Xue M, Yang C, Wang P, Yang Y, Zhu H, Wu C, Yao Y, Luo W, Zou Z: **Faradaic junction and isoenergetic charge transfer mechanism on semiconductor/semiconductor interfaces**. *Nat Commun* 2021, **12**:1–8, https://doi.org/10.1038/s41467-021-26661-6. 12 (2021).

[57]. ** Wang P, Xue M, Jiang D, Yang Y, Zhang J, Dong H, Sun G, Yao Y, Luo W, Zou Z: **Photovoltage memory effect in a portable Faradaic junction solar rechargeable device**. *Nat Commun* 2022, **13**, https://doi.org/10.1038/s41467-022-30346-z.

They devised a real-time step wise open circuit potential method of probing an observed mechanism of the Faradaic junction i.e. a photo-voltage memory during dark discharge. They found a minimised energy loss at the interface meaning increased performance. They also created a device that returned the highest dark volumetric energy density of any recorded two-electrode high-rate photoelectrochemical device. Using the prerequisite they propose will enable future devices to be created.

[58]. Lee J, Lee DM, Jung Y, Park J, Lee HS, Kim YK, Park CR, Jeong HS, Kim SM: **Direct spinning and densification method for high-performance carbon nanotube fibers**. *Nat Commun* 2019, **10**:1–10, https://doi.org/10.1038/s41467-019-10998-0. 10 (2019).

[59]. Zhang J, Jiang D, Wang P, Zhong J, Sun G, Yao Y, Luo W, Zou Z: **A high-voltage solar rechargeable device based on a CoPi/BiVO4 faradaic junction**. *J Mater Chem A Mater* 2022, **10**:1802–1807, https://doi.org/10.1039/d1ta08949h.

[60]. Roy A, Majumdar P, Sengupta P, Kundu S, Shinde S, Jha A, Pramanik K, Saha H: **A photoelectrochemical supercapacitor based on a single BiVO4-RGO bilayer photocapacitive electrode**. *Electrochim Acta* 2020, **329**, 135170, https://doi.org/10.1016/j.electacta.2019.135170.